WHOI-88-31

Woods Hole Oceanographic Institution

The Release and Migration of Activation Products of Corrosion-Resistant Metal Specimens in Marine Sediments

by

L.A. Ball and F.L. Sayles

August 1988

Technical Report

WHOI-88-31

The Release and Migration of Activation Products from Corrosion-Resistant Metal Specimens in Marine Sediments

by

L.A. Ball and F.L. Sayles

Woods Hole Oceanographic Institution
Woods Hole, Massachusetts 02543

August 1988

Technical Report

Approved for Distribution:

Frederick L. Sayles, Chairman
Chemistry

INTRODUCTION

1. Previous Work:

This experiment was designed to measure the release and migration of the neutron-activated radionuclides, Ni-63, Co-60, and Fe-55, from two types of corrosion-resistant alloys, Inconel-600 and SS-347 into marine sediments. A previous report[1] described the experimental design in detail. To briefly summarize, on 11 August 1982 we deployed six 50 cm long probes at Deep Ocean Site 2 (DOS-2). Each probe held 5 metal specimens such that each specimen would be exposed to sediment at depths of approximately 3, 7, 15, 25, and 40 cm. Three probes held Inconel-600 specimens and three held SS-347. On July 17, 1983, we recovered one probe of each type of metal (probes #3 and #5). The extrusion and subsectioning procedure as well as the analytical methods and results from these cores were described in detail in the previous report. The integrated release rates for the three nuclides fell between 0.02-13 $nCi/cm^2/yr$ for Inconel-600 and 0.007 to 0.36 $nCi/cm^2/yr$ for SS-347. Estimated diffusion coefficients were between 10^{-8} and 10^{-9} cm^2/sec for the three nuclides. We noted difficulty in detecting Fe-55 in general due to its short half life and consequently low specific activity. Measurement of Ni-63 in the core containing SS-347 foils was also difficult due to the low nickel content of this alloy and the relatively high detection limit of the LSC method.

2. Current Work:

The previously-noted difficulty in measuring Ni-63 was due, essentially, to the large background and high detection limit for the liquid scintillation counting method. In attempting to improve the detection limit for Ni-63, we have developed a windowless, Geiger-Mueller type beta counter.

The four remaining probes (#1, #2, #4, and #6) were overcored in late June and early July 1986. Extrusion and horizontal subsampling of the cores was carried out according to the following schedule:

Core/Probe #4, Inconel-600	27 June 1986
Core #6, Inconel-600 (no probe)	29 June 1986
Core/Probe #1, SS-347	1 July 1986
Core/Probe #2, SS-347	1 July 1986

Using 27 June 1986 as an average recovery date, the elapsed time from the 11 August 1982 deployment was 1418 days (3.882 years). Note that Probe #6 was not recovered with its overcore. This core was extruded in approximately 5 cm thick by 5 cm radius bulk sections. Cores #1, #2, and #4 were extruded in 2 cm vertical sections and subsampled horizontally with syringes and refrigerated. The syringes were sampled in 2 mm sections in the laboratory in Woods Hole. A total of over 2300 two-millimeter samples were generated from the three intact cores.

Pore water samples characterizing the redox chemistry of the sediments were taken with both an Alvin deployed instrument (WHIMPER) and from push cores squeezed in the ship's lab (Whole Core Squeezer).

METHODS

1. Development of a Windowless G-M Counter for the Measurement of Ni-63:

Introduction

A previous report[1] described measurements made of Ni-63 in sediments using the liquid scintillation counting (LSC) method. It was noted that the analytical limits of this method were approached preventing an accurate tracking of the Ni-63, signal especially for cores containing the low nickel content alloy SS-347. In an attempt to extend this detection limit, a beta counter with more optimal counting characteristics has been developed. Ni-63 decays with the exclusive emission of a low energy beta particle (E max = 67 kev). Traditional thin window Geiger-Muller (G-M) counters are inefficient at counting such low energy beta particles due to absorption by the entrance window. The detector described below is a windowless design that overcomes the shortcomings of both the LSC and the thin window G-M counters.

Design

The physical configuration of the counter body was patterned after designs reported in the literature for thin window detectors[2,3]. The counter, as shown in Figure 1, was constructed of clear acrylic sheet (0.25" thickness). Assembled, the counter measures approximately 2.5"x3.0"x4.5". It contains 4 separate detectors. The cathodes, upon which the nickel sources are electroplated, are copper discs (1" diameter x 0.016" thick). Each pair of cathodes is mounted on a removable shelf which is O-ring sealed against the outer edge of the counting chamber. The anode wires are 1 mil thick #304 stainless steel. Connection of the anodes to a high voltage source and the cathodes to ground is made through 4 MHV connectors mounted on the counter body. Serial gas connec-

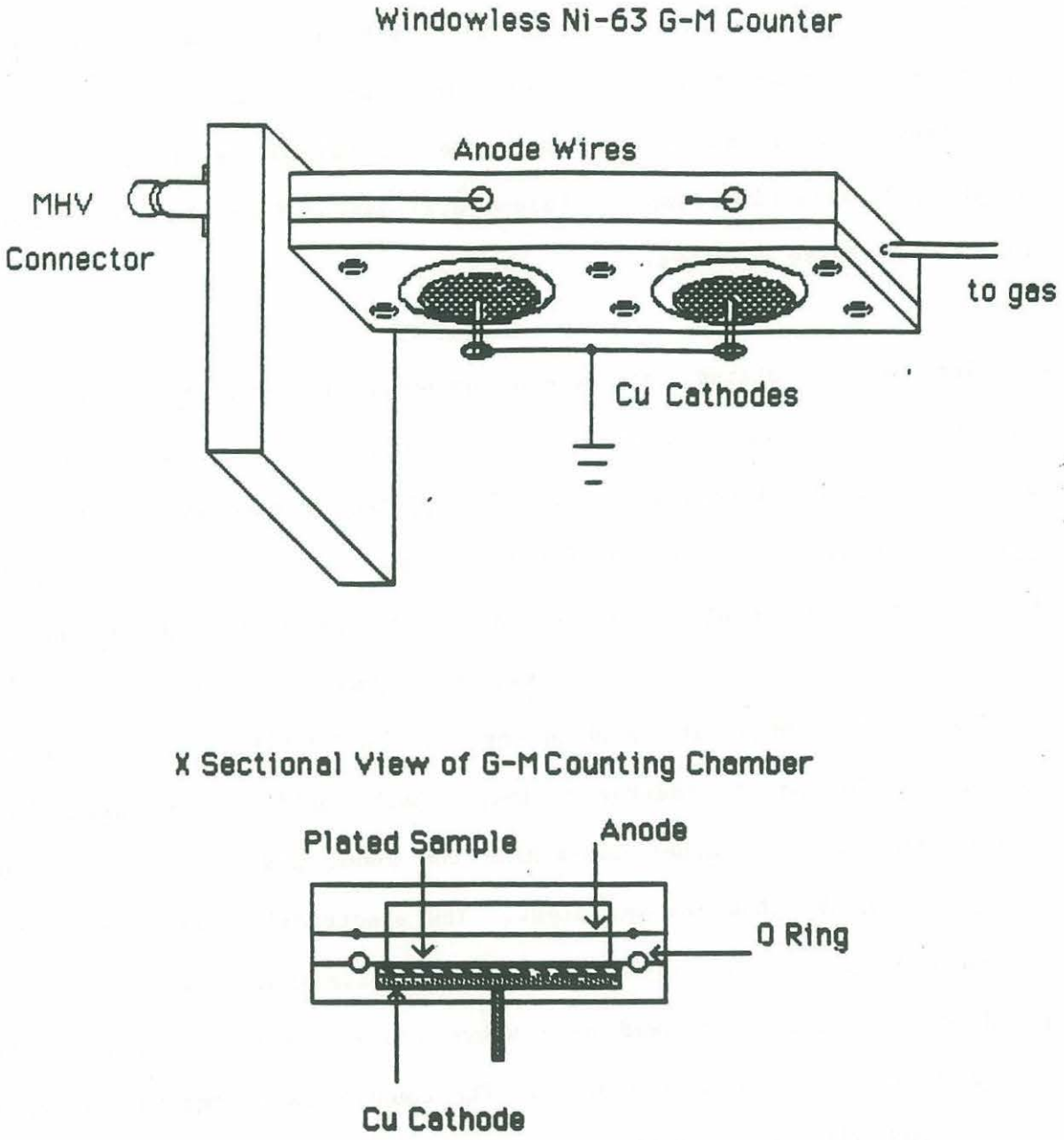

Figure 1. Windowless G-M Counter for Ni-63 Measurement.

tions through all 4 detectors are machined into the counter body.

The electronic circuitry has been described elsewhere[3] and is standard for G-M counters. The counter was designed to operate within an existing shield of anticoincidence detectors which is essentially a ring of G-M counters constructed of brass tubes. The anticoincidence circuitry blocks the counting of pulses that are detected at both the A/C shield and the primary detectors within a defined time window. Pulses originating from the sample counter are recorded on pulse counters.

Operation

Samples are plated onto clean copper discs from a concentrated NH_4OH solution that is approximately 0.5 N NH_4SO_4 at 0.1 A for 2 hours with a 0.5 cm anode to cathode distance. The plated Ni adheres well to the copper planchet and appears to be evenly distributed. After plating, residual stable Ni is determined by atomic absorption spectrometry in order to quantify the plating yield. Plating yields are typically greater than 95%.

The plated samples are mounted for counting by first placing the planchets on the cathodes on the counter shelves. Each shelf is then carefully positioned beneath the chamber containing the anode and is snugged against the O-ring making the chambers gas tight. The electrical ground connections from the cathode to the MHV connectors are then attached. The counter is placed inside the AC shield and lead cave where the gas and electrical connections are made to the external equipment. The counter is purged with counting gas (99.05% helium/0.95% isobutane or Q gas) at about 1-2 ml per minute overnight before the bias voltage is applied. The high voltage is applied slowly and allowed to stabilize several minutes before counting is started. The count rate is monitored periodically to note the presence of short-lived contamina-

tion or the occurrence of spurious counts. Counting data are considered valid when two or more overnight consecutive counts agree to within ±2 sigma error limits.

Calibration

The first step in calibrating the detectors was to establish the bias voltage plateau. This is a range of voltage over which the counting efficiency varies only slightly. When the detector is operated at the midpoint of this voltage range, slight drift in bias voltage has a negligible effect on the counting efficiency. Below the plateau voltage, the efficiency is very low; above it, the detector continuously discharges and damages the anode. Ideally, the plateau is 100 volts or more and has a slope of 1-2% or less. Early in their lifetimes, the detectors functioned well and were calibrated with Ni-63 sources of different thicknesses of stable Ni to correct for self absorption of the 67 kev beta particle. Figure 2 shows a self-absorption correction curve prepared for one of the detectors. Curves for the other detectors are similar but are unique to each detector. Standards were prepared by plating varying amounts of stable nickel with a known amount of Ni-63 and correcting for plating loss by AA measurement of the postplating solution. The working area of the curve is generally between 1 and 4 mgs of nickel giving counting efficiencies between 10 and 18 percent. Background count rates measured for blank copper discs varied between 0.056 ± 0.004 cpm and 0.098 ± 0.005 cpm for different detectors (3-day counts).

Using the following equation defining detection limit from Volchok and Deplanque[4]:

$$LLD = [4.66 * Ebkg]/[Eff * Rec]$$

where:

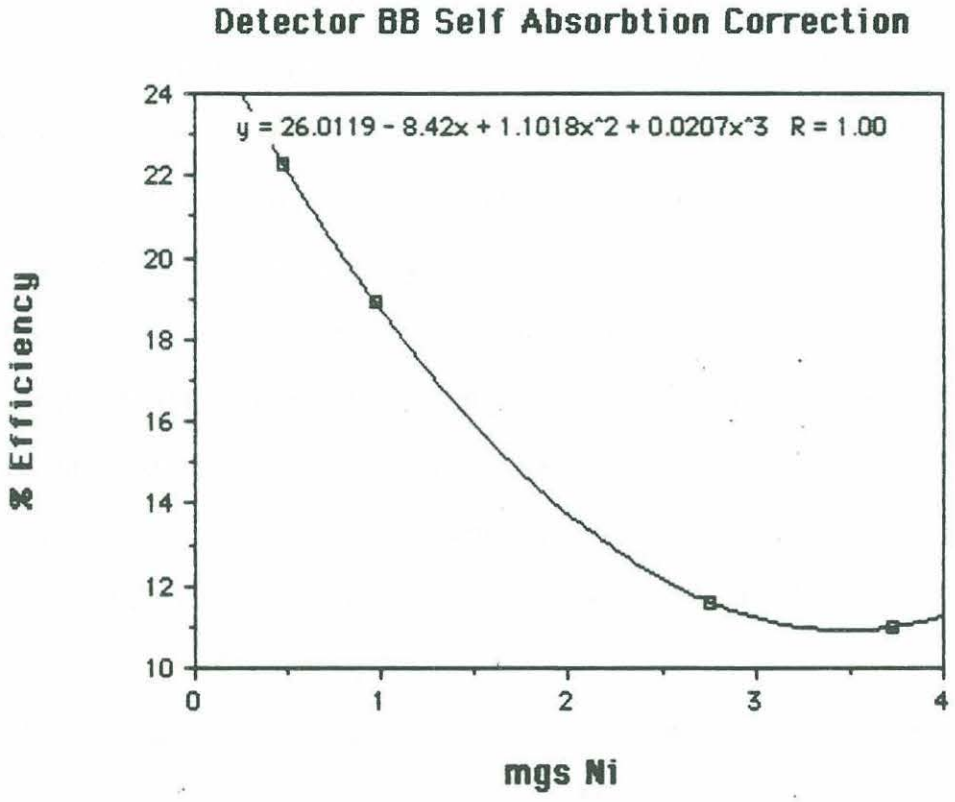

Figure 2. Self-absorption plot for Ni-63 plated with stable nickel. The detection efficiency of the 67 kev Ni-63 beta particle is plotted as a function of the mass of the plated stable nickel.

LLD = lower limit of detection (2 sigma error)

Ebkg = 1 sigma error in background count rate

Eff = detector efficiency

Rec = fractional overall chemical recovery

For comparison, these factors for LSC and Windowless G-M counting of Ni-63 are listed in the following table:

Table 1.

Comparison of Detection Limits for LSC and G-M Counting Ni-63

Counter	Time (min)	BKG (cpm)	E bkg	Eff (%)	Rec (%)	LLD (dpm)
LSC	1000	30	0.2	60	90	2
LSC	5000	30	0.08	60	90	0.7
G-M	1000	0.06	0.008	15	90	0.3
G-M	5000	0.06	0.003	15	90	0.1

By using the G-M counter, the detection limit is improved by nearly an order of magnitude for a relatively short counting period (1000 mins.). Since the windowless counter provides 4 detectors as opposed to a single LSC detector, longer counting periods can be justified. The detection limit for the 5000 minute counting period is 20X lower than the limit for the 1000 minute count on the LSC.

Performance

G-M counters are notoriously sensitive devices and the windowless type is especially prone to contamination of the chamber and degradation of the anode. Three of the four detectors in the counter have been successfully calibrated. The performance of the fourth has been consistently bad. Two of the three "good" detectors underwent replacement of their anodes early in their development. Following the anode replaement, useful calibrations were obtained for three of the four detectors, and an attempt was made to measure Ni-63 in sediment samples.

Core #6 was recovered with loss of its Inconel-600 probe and was extruded in 5 cm thick by 5-6 cm radius sections. It provides a good source of Ni-63 spiked sediment. Nickel fractions from acid leaching of sediment from 4 sections were plated onto copper planchets and counted on the windowless counter. Three of the four samples were recounted on different detectors to obtain a measure of the effect of the error in correcting for self-absorption on the precision of the measurement. As it turned out, the intercomparison showed the onset of instability in the detectors. The following table shows the results of these measurements:

Table 2.

Sample Section	Ni-63 (dpm/g) Count #1	Count #2	% Difference
0-5 cm	3224 ±9	3308±8	2.5
5-10 cm	106 ±2	117±3	9.4
10-16 cm	28 ±1	38±2	26.3
16-21 cm	15.1±0.7	--	--

Comparison of the per cent differences in recounts shows that the counters were not stable with respect to counting efficiency. We attempted to recount the self-absorption standards and found the absolute counting efficiency to have decreased by 2% or more, and the detectors to have drifted to the point where a new and higher voltage plateau needed to be determined. Repeating the plateau determination only provided a temporary solution. It soon became evident from the lack of stability in the counting efficiency and the fact that the plateau was occurring at an ever higher voltage and extending over a shorter voltage range that the detectors had worn out. This behavior was experienced earlier prior to the replacement of the electrodes in two of the detectors and was attributed to exceeding the plateau voltage and operating at continuous discharge. Continuous discharge can occur because the detectors require a period of "burning in" during which they are subjected to a high voltage just short of continuous discharge. After this, they operate at a lower plateau voltage than would have been possible without the burning process. Without knowing the point at which they discharge, it is easy to push the voltage too high. Occasionally, a detector will operate for a period of days before going into continuous discharge spontaneously. We believe the lifetime of the anode is related to the frequency and duration of the periods that it is operated at continuous discharge. Although the data set is limited, we can estimate a lifetime of about 5 months for this type of detector which, having gained experience in its operation, could possible be extended by minimizing the operation at continuous discharge.

Conclusions

A new type of windowless G-M beta counter for the low level determination of Ni-63 has been described. The counter has been built and successfully

calibrated demonstrating an improvement in detection limit of about 10X to 20X over the liquid scintillation technique primarily due to a substantial reduction in background when operated within an anticoincidence shield and lead cave. Deterioration of the counter as evidenced by decreased counting efficiencies prevented use of the counter to measure sample activities of Ni-63. The lifetime of the detectors was about 5 months. Degradation of the anode due to operation at continuous discharge as well as a general vulnerability due to the windowless design probably lead to such a short operating lifetime.

2. Analytical Techniques:

The routine analysis of the sediment samples was conducted using the methods reported previously with a few exceptions. One set of analyses of Core #6 was done on samples weighing several grams. Due to the inclusion of an excessive amount of magnesium salts in the nickel fraction, a nickel-dimethylglyoxime precipitation was done to remove the magnesium contamination. All Ni-63 samples were counted on a new Packard Model 4350 B liquid scintillation counter at an efficiency of 64.4% using a 0-67 kev window.

Co-60 samples were mounted as cobalt ammonium phosphate ($CoNH_4PO_4.H_20$) and counted on thin window G-M counters as before. All detectors were recalibrated for Co-60 counting.

Fe-55 was difficult to detect in the 1983 sample set. A method with a lower detection limit than our previously reported method was not found. The additional four years of decay time for a nuclide with a 2.6 year half life compounded the problem of measuring Fe-55.

RESULTS AND DISCUSSION

1. Chemical Environment:

Changes in redox potential in pelagic sediments such as found at the DOS-2 site are mediated by the biological utilization of the most energetically favorable oxidizer of organic material. They are in order of utilization: O_2, NO_3^{-1}, MnO_2, SO_4^{-2}, and Fe^{+3}. In the report of the data from the July 1983 recoveries, we discussed the measurements of some of these chemical redox indicators which essentially defined the following redox zones:

0–4 cm	O_2 present at surface, falling to zero at 3–4 cm; nitrification occurring.
4–12 cm	NO_3^{-1} reduction occurring.
12–>20 cm	MnO_2 reduction occurring; Mn^{+2} present.
>20 cm	Not sampled.

The results of our pore water analyses from the June/July 1986 cruise are summarized in Figure 3. This plot of total (NO_3^{-1}+NO_2^{-1}) or (N+N) combines two data sets: points covering the upper 3.5 cm are from squeezing a 2.5 inch diameter core on deck, the lower data points are from pore water samples taken at depth with the WHIMPER by the ALVIN. The close sampling of the upper 3.5 cm clearly delineates the nitrification process as shown by the increase of N+N from 22 to 32 uM/L in the 0–1 cm interval. the presence of O_2 is inferred by nitrification, and O_2 is probably not depleted until between 3.5 and 5 cm where total N+N is declining rapidly. By 10 to 12 cm N+N is undetectable signifying the onset of MnO_2 reduction to Mn^{+2}. This detailed N+N profile compares well with our results from 1983 and leads us to believe no substantial temporal changes in redox chemistry have taken place.

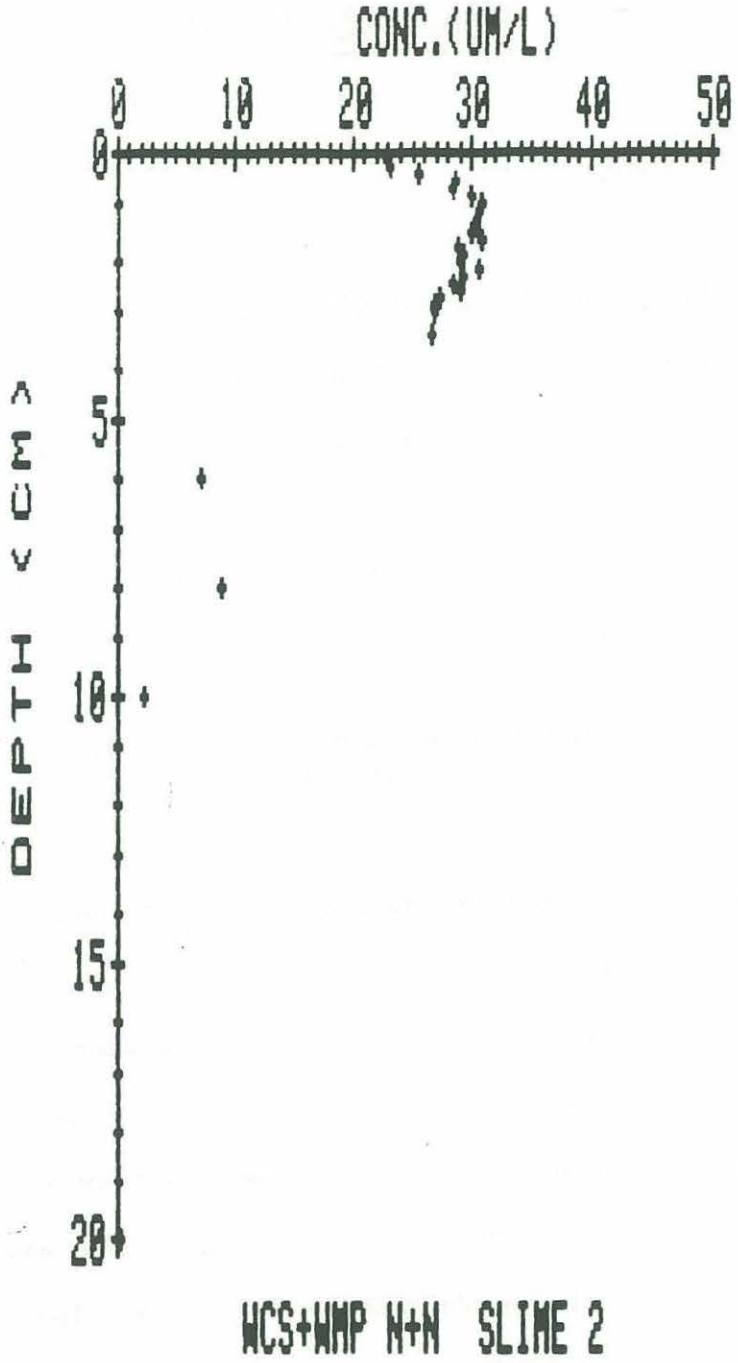

Figure 3. Total (NO_3^-+NO_2^-) concentration is plotted as a function of the depth below the sediment water interface for DOS-2 sediments.

2. Counting Data:

Fe-55 Activities

Fe-55 with a half life of 2.7 years has decayed to very low levels in the sediments. Our analyses of Cores #3 and #5 in 1983 gave detectable activities in only a relatively few instances despite measurable release rates from the foils as estimated from the Ni-63 and Co-60 data. We anticipated even more difficulty with the samples taken in 1986 given the additional 3-4 years of decay time. In order to evaluate the practicality of measuring Fe-55, we chose to analyze 3 samples from Core #4 for Fe-55. These had the highest levels of Ni-63 and Co-60 of the 3 intact cores. We are aware that the Fe-55 content of the Inconel-600 foils from this core (19 uCi/foil) are less than that of the SS-347 foils (118 UCi/foil) but felt that the increased release rate from the Inconel allow over the SS-347 as previously reported would more than compensate for this. The activities for these samples and a reagent blank are as follows:

Table 3.

Sample	Fe-55 (cpm±1S)
Background	1.11 ± 0.02
Rgt Blank #1	1.00 ± 0.02
Core #4, 6-8 cm N, 0-2 mm	1.29 ± 0.02
Core #4, 6-8 cm N, 2-4 mm	1.29 ± 0.02
Core #4, 8-10 cm E, 0-2 mm	1.28 ± 0.02

The sample activities lie very close to background and blank levels. Clearly, if these are the highest level samples, it would serve no purpose to continue to analyze an extended array of blank or nearly blank samples. Instead, we devoted our effort to defining the behavior of the Ni-63 and Co-60.

Co-60 and Ni-63 Activities

Tables 4, 5, 6, and 7 show the activites of Co-60 and Ni-63 as of the dates of counting for the four cores. Referring to these, we can comment on the general quality of the data for each core.

Core #1, SS-347: Table 4

Of the three cores recovered with probes, Core #1 probably was disturbed the most. From notes made during extrusion we were able to locate the sediment horizons that were in proximity to the SS-347 foils. The core did not recover sediment lying as deep as the lowest foil. The 16-18 cm and 24-26 cm horizons show high activities of Ni-63 and Co-60 and verify our estimates of the positions of the foils relative to the sediment. The upper 2 sections, however, have lower activities of Ni-63 and Co-60 than we would expect. The horizontal profiles of these two sections strongly suggest admixture of unlabeled sediment either during coring or recovery.

Table 4.

Sample I.D., location in the core, dry sample weight, Ni-63 and Co-60 activities in dpm/g as of the counting date and the associated one sigma counting errors for Core #1.

Core#1 Co-60 and Ni-63 Activities as of Count Date

VIAL #	VERT (CM)	HORIZ (MM)	DRY WT (G)	Co-60 (dpm/g)	Error (1S)	Ni-63 (dpm/g	Error (1S)
1-1	0-2 N	0-2	0.1619	1.1	0.4	4	8
1-2	"	2-4	0.0941	4.4	0.7	12	21
1-3	"	4-6	0.0909	5.0	0.7	2	21
1-4	"	6-8	0.1146	4.9	0.6	-1	17
1-138	6-8 N	0-2	0.1452	2.4	0.4	20	13
1-139	"	2-4	0.1227	0.6	0.5	10	16
1-140	"	4-6	0.1566	1.0	0.4	-2	13
1-141	"	6-8	0.1348	0.3	0.5	-1	15
1-278	14-16 NE	0-2	0.1924	457	1	117	7
1-279	"	2-4	0.2559	42.5	0.4	3442	37
1-280	"	4-6	0.1731	13.8	0.5	33	12
1-281	"	6-8	0.1794	10.4	0.5	44	11
1-447	24-26 N	0-2	0.2344	190	1	535	10
1-448	"	2-4	0.1886	66.5	0.6	77	10
1-449	"	4-6	0.1989	42.7	0.6	34	10
1-450	"	6-8	0.2161	25.9	0.5	25	11

Core #2, SS-347: Table 5

Core #2 was recovered relatively intact and has measurable activities of Ni-63 and Co-60 at all depths corresponding to foils. Some extra analyses were done to find sections with the highest close-in activities. The 6-7.5 cm and 12-14 cm sections show a curious feature of a peak in activity 2 to 4 mm out from the initial horizontal sections. We have seen this in other core sections and cannot offer an explanation other than unverified physical displacement.

Table 5.

Sample I.D., location in the core, dry sample weight, Ni-63 and Co-60 activities in dpm/g as of the counting date and the associated one sigma counting errors for Core #2.

Core#2 Co-60 and Ni-63 Activities as of Count Date

VIAL#	VERT CM	HORIZ MM	SAMPLE DRY	Co-60 (dpm/g)	Error (1S)	Ni-63 (dpm/g)	Error (1S)
2-029	2-4 N	0-2	0.0926	14.4	0.6	38	17
2-030	"	2-4	0.1152	9.5	0.7	25	14
2-031	"	4-6	0.1013	5.4	1.0	13	16
2-033	"	8-10	0.09625	-2.5	0.6	9	17
2-075	4-6 N	0-2	0.1048	4.4	0.6	7	14
2-118	6-7.5 N	0-2	0.0929	30.0	0.8	76	17
2-119	"	2-4	0.1251	41.3	1.1	82	13
2-120	"	4-6	0.15948	5.3	0.5	37	11
2-122	"	8-10	0.11841	2.0	0.6	10	14
2-162	7.5-9.5 N	0-2	0.1650	34.4	0.3	42	10
2-180	7.5-9.5 S	0-2	0.1638	9.5	0.3	11	10
2-193	9.5-12 N	0-2	0.2160	5.7	0.3	8	7
2-232	12-14 N	0-2	0.1896	81.6	0.6	66	5
2-233	"	2-4	0.1228	126	1	96	9
2-234	"	4-6	0.14393	291	2	327	9
2-235	"	6-8	0.1296	71	1	42	6
2-236	"	8-10	0.13642	48	1.0	41	9
2-271	14-16 N	0-2	0.2247	25.4	0.2	15	5
2-399	22-24 N	0-2	0.1657	44.9	0.3	88	10
2-400	"	2-4	0.1723	8.6	0.5	26	10
2-401	"	4-6	0.17565	5.4	0.5	10	10
2-402	"	6-8	0.2214	4.8	0.4	16	8
2-403	"	8-10	0.21869	6.1	0.4	2	8
2-438	24-26 N	0-2	0.3022	26.1	0.2	66	9
2-677	36-38 N	0-2	0.1624	0.9	0.4	-1	11
2-716	38-40 N	0-2	0.1526	8.1	0.3	2	11
2-717	"	2-4	0.1785	6.3	0.4	11	10
2-718	"	4-6	0.0951	6.4	0.8	5	19

Core #4, Inconel-600: Table 6

Core #4 was probably the least disturbed core as judged by its appearance and the minimal cratering around the probe at the sediment surface and, hence, was the most extensively analyzed. In our 1983 report, we did not measure any blank values of Co-60. For this core we felt it important to extend the Co-60 analyses horizontally until we reached blank or constant values which would signify a blank contribution. Happily, we can demonstrate activities at the background level of the detectors in the case of several of Core #4's sections assuring us of the lack of a blank contribution to the Co-60 analyses from the unlabeled sediment. Interestingly, the horizontal displacement of activity maxima outward from the initial sample are really quite infrequent and of a small magnitude in this core. The extensive data set and its undisturbed condition of Core #4 make its results the most conclusive of all the cores.

Table 6.

Sample I.D., location in the core, dry sample weight, Ni-63 and Co-60 activities in dpm/g as of the counting date and the associated one sigma counting errors for Core #4.

CORE#4 CO-60 AND NI-63 ACTIVITIES AS OF COUNT DATE

VIAL #	VERT CM	HORIZ MM	SAMPLE WT (GMS)	Co-60 (dpm/g)	Error (1S)	Ni-63 (dpm/g)	Error (1S)
4-055	4-6 E	0-2	0.0901	13.5	0.8	N.A	--
4-057	"	4-6	0.1003	4.4	0.6	N.A.	--
4-059	"	8-10	0.1152	5.6	0.5	N.A.	--
4-061	"	12-14	0.1184	-1.1	0.6	N.A.	--
4-063	"	16-18	0.1014	0.5	0.4	N.A.	--
4-065	"	20-22	0.1015	5.6	0.6	N.A.	--
4-067	"	24-26	0.1021	1.3	0.5	N.A.	--
4-069	"	28-30	0.1013	1.3	0.5	N.A.	--
4-142	6-8 E	0-2	0.13	18.4	0.5	N.A.	--
4-144	"	4-6	0.15	4.2	0.4	N.A.	--
4-146	"	8-10	0.12	3.4	0.4	N.A.	--
4-148	"	12-14	0.15	6.2	0.4	N.A.	--
4-152	"	20-22	0.1150	0.7	0.5	N.A.	--
4-154	"	24-26	0.1588	0.9	0.5	N.A.	--

Table 6. (Cont.)

VIAL #	VERT CM	HORIZ MM	SAMPLE WT (GMS)	Co-60 (dpm/g)	Error (1S)	Ni-63 (dpm/g)	Error (1S)
4-156	6-8 N	0-2	0.10	417	8	10070	101
4-157	"	2-4	0.1542	261	1	7746	75
4-158	"	4-6	0.15	34.1	0.7	3221	36
4-159	"	6-8	0.1366	10.0	0.5	868	15
4-160	"	8-10	0.15	5.6	0.5	130	12
4-162	"	12-14	0.15	4.9	0.4		--
4-164	"	16-18	0.1005	-0.1	0.5	222	16
4-166	"	20-22	0.1363	-1.6	0.5	N.A.	--
4-168	"	24-26	0.1424	0.4	0.5	N.A.	--
4-170	"	28-30	0.0876	2.1	0.8	N.A.	--
4-216	8-10 E	0-2	0.1779	280	1	2084	24
4-217	"	2-4	0.1631	4.6	0.4	1412	13
4-218	"	4-6	0.1485	16.6	0.5	99	12
4-219	"	6-8	0.1569	1.2	0.4	324	11
4-220	"	8-10	0.1459	0.6	0.4	-2	11
4-222	"	12-14	0.1462	0.1	0.4	N.A.	--
4-224	"	16-18	0.1706	-1.5	0.4	N.A.	--
4-228	"	24-26	0.1174	1.3	0.5	N.A.	--
4-262	10-12 E	0-2	0.1474	347	1	822	15
4-263	"	2-4	0.1523	6.0	0.4	24	11
4-264	"	4-6	0.1666	7.5	0.4	4	10
4-265	"	6-8	0.1870	4.0	0.3	3	9
4-266	"	8-10	0.1606	1.4	0.4	13	11
4-412	16.5-18.5	0-2	0.1532	14.1	0.5	41	11
4-414	"	4-6	0.1790	11.1	0.5	31	10
4-416	"	8-10	0.1565	9.8	0.5	14	11
4-418	"	12-14	0.2339	7.2	0.5	12	7
4-420	"	16-18	0.1631	4.7	0.5	0	7
4-422	"	20-22	0.1627	2.7	0.4	N.A.	--
4-424	"	24-26	0.2661	2.5	0.3	N.A.	--
4-426	16.5-18.5	2-4	0.2179	8.4	0.4	N.A.	--
4-463	18.5-20.5	0-2	0.1819	6.3	0.4	N.A.	--
4-568	25.5-27.5	0-2	0.2261	19.8	0.5	271	9
4-570	"	2-4	0.1770	6.4	0.5	37	9
4-572	"	8-10	0.1774	5.2	0.4	22	10
4-574	"	12-14	0.1665	3.0	0.4	14	10
4-576	"	16-18	0.1646	0.9	0.4	N.A.	--
4-578	"	20-22	0.1826	1.2	0.3	N.A.	--
4-580	25.5-27.5	0-2	0.1010	-0.1	0.5	N.A.	--
4-622	27.5-29.5	0-2	0.1135	117	1	610	16
4-623	"	2-4	0.1648	7.2	0.4	2	10
4-624	"	4-6	0.1408	3.5	0.3	-1	12
4-625	"	6-8	0.1660	2.3	0.4	-5	10
4-774	41-43 E	0-2	0.1461	4.3	0.4	14	11
4-776	"	4-6	0.1574	2.6	0.4	5	10
4-777	"	6-8	0.1785	1.5	0.4	4	10
4-779	"	10-12	0.2087	0.8	0.4	3	8
4-781	"	14-16	0.1815	1.6	0.3	-2	9
4-783	"	18-20	0.1608	0.8	0.3	-10	11
4-832	43-45 SE	0-2	0.1989	3.0	0.3	N.A.	--

Core #6, Inconel-600: Table 7

Core #6 was recovered without a probe. This was noticed only after surfacing from the ALVIN dive. The likely cause was underpenetration of the corer which left the bottom end of the probe protruding. The notch holding the bottom Inconel foil could then have hung up on the edge of the basket and drawn the probe through the core as it was lifted into the core quiver. The surface of Core #6 showed a trench running from the center to the outer edge of the core suggesting the probe was forced horizontally as it was drawn out of the core. As previously mentioned, Core #6 was extruded in 5 cm radius by 5 cm thick sections centered about the original location of the probe. The sections were mixed by hand before subsampling for analysis.

Table 7.

Ni-63 and Co-60 activities for Core #6. Results for 3 aliquots from each vertical section are listed. For Ni-63, purification of the nickel fraction by DMG precipitation is noted when done.

CORE#6: NI-63 AND CO-60 ACTIVITIES AS OF COUNTING DATE

Sample	Ni-63 A.	Ni-63 B.	Ni-63 C.	Ni-63 mean	Co-60 A.	Co-60 B.	Co-60 C.	Co-60 mean
NOTE:	no DMG ppt'n	DMG ppt'n	DMG ppt'n	+_1 std. dev.				+- 1 std. dev.
0-5 cm	3493+-170	1963+-100	2190+-100	2551+-824	91.7+-0.2	62.5+-1.3	110+-2	91+-28
5-10 cm	319+-11	95+-5	74+-4	163+-136	11.8+-0.1	15.3+-0.3	14.0+-0.3	14+-2
10-16 cm	61+-2	22+-1	12+-1	32+-26	19.3+-0.1	16.8+-0.3	16.9+-0.3	18+-1
16-21 cm	21.2+-1.6	3.4+-0.2	9.0+-0.5	11+-9	4.6+-0.2	4.63+-0.09	4.20+-0.09	4.5+-0.2

As Table 7 shows, two nickel fractions from 5-8 gram (wet weight) subsamples were purified from magnesium contamination with a dimethylglyoxime precipitation before analysis. One nickel fraction from a 0.5 g subsample was analyzed without purification. The nickel activities of purified vs. unpurified subsamples suggest a radioactive component removable by the dimethylglyoxime precipitation. The Co-60 activities of the different subsamples, all analyzed identically, show a significant inhomogeneity in the bulk sample as might be expected from the mixing method. This inhomogeneity obscures the evaluation of a contaminant being present in the nickel fraction. We have used the mean value of these data in subsequent calculated results such as release rates. The error in the mean values reflects the substantial spread in the data. The activities are maximum at the top section and fall off steeply with depth. This is also the case with Core #4 (also an Inconel core), but not so with Cores #1 and #2 (SS-347 cores). The implications in terms of release rates versus redox regime and allow type are discussed in the section on integrated release rates.

3. Integrated Activities Released and Rates of Release:

Integrated activities released (AR) and release rates (RR) for the three cores sampled in 2 mm horizontal sections were calculated using the following equations and rationale:

$$AR = [A * D * B * VS * F] / W:D$$

where:

AR = Activity Released (nCi)

A = Activity of a 2 mm section (dpm/g dry)

D = Decay Factor correcting activity to deployment date: 11 August 1982

B = Bulk Density (g/cm^3 wet)

VS = Volume of a sediment shell 2 mm thick of a radius equal to the distance from the probe of the horizontal section taking into account the volume occupied by the probe

F = A conversion factor from dpm to nCi (2.22×10^3 dpm/nCi)

W:D = Wet to dry weight ratio

The total activity released for an individual vertical horizon is the sum of the AR values for all the 2 mm sections in that vertical section.

The release rate (RR) can be calculated for each foil as:

$$RR = AR/(SA * T)$$

where:

RR = Release Rate (nCi/cm^2/yr)

AR = Activity Released (nCi) summed for a 2 cm vertical section

SA = Surface Area of foil specimen (1.081 cm^2)

T = Elapsed time between deployment and recovery (3.882 years)

These calculations assume a uniform spherical distribution of activity as characterized by our determinations on samples taken horizontally from the source. This probably underestimates the integrated activities as we see higher activities in samples taken 2 cm vertically from a foil than we would expect from activities measured an equal distance horizontally. That is to say there may be enhanced migration vertically along the probe that we were not in a position to evaluate. It should also be stressed, as it was in the 1986 report, that release rates are not to be construed as corrosion rates. We have sampled only that activity that has migrated away from the foil specimen and not that which may have corroded from it but still remains in proximity to its surface.

To comment on the activities released and release rates for the four cores:

Core #1, SS-347: Table 8

AR and RR are poorly characterized in the upper two sections due to low Ni-63 and Co-60 activities. For both the 14-16 cm and 24-26 cm sections, the Co-60 release rates fall around 0.08 $nCi/cm^2/yr$. This compares with values of 0.05 $nCi/cm^2/yr$ (16-18 cm) and 0.07 $nCi/cm^2/yr$ (42-44 cm) reported for Core #3 collected in 1983. The Ni-63 release rates in the lower sections are 0.5 $nCi/cm^2/yr$ for 14-16 cm and 0.06 $nCi/cm^2/yr$ for 24-26 cm. Core #3, from the 1986 report gave 0.01 to 0.007 for 3 sections at 16 cm and lower. 94% of the 0.5 $nCi/cm^2/yr$ value for the 14-16 cm depth is derived from the 2-4 mm sample. The cobalt activity is not similarly inflated, leading us to consider this value suspect, at least to the point of reflecting an abnormal process such as incorporation of physically displaced solid corrosion products.

Table 8.

Integrated Activities Released (AR) and Integrated Release Rates (RR) of Co-60 and Ni-63 for various vertical sections of Core #1. (N.D. = Not Determined)

Depth (cm N)	Co-60 AR(nCi) ± 1 S	Co-60 RR($nCI/CM^2/yr$) ± 1 S	Ni-63 AR(nCi) ± 1 S	Ni-63 RR($nCI/CM^2/yr$) ± 1 S
0-2	0.0167 0.0014	0.0040 0.0003	N.D.	
6-8	0.0025 0.0014	0.0006 0.0003	0.0032 0.0014	0.0008 0.0003
14-16	0.3432 0.0018	0.0818 0.0004	2.0770 0.0284	0.4949 0.0068
24-26	0.3167 0.0018	0.0755 0.0004	0.2595 0.0180	0.0618 0.0043

Core #2, SS-347: Table 9

Core #2 shows low release rates of Co-60 in the upper sediment sections of 0.005 to 0.015 nCi/cm^2/yr reaching a maximum at 12-14 cm of 0.22 nCi/cm^2/yr. The release rate then falls off at deeper depths to its initial surface value of 0.005 nCi/cm^2/yr at 38-40 cm. In the SS-347 core reported on in 1986 (Core #3), we noted maximum values of 0.3-0.4 nCi/cm^2/yr in the 4-6 cm and 8-10 cm sections.

Ni-63 follows a pattern of release rate with depth similar to Co-60 reaching a maximum of ~0.11 nCi/cm^2/yr in the 12-14 cm section. The Ni-63 data from Core #3 show a maximum near the surface that falls off steadily with depth. The values of the maximum release rates compare well: 0.11 nCi/cm^2/yr for Core #2 vs. 0.085 nCi/cm^2/yr for Core #5 the 4-6 cm section. The discrepancy between the location of the maxima begs the question of whether release is accelerated in the presence of O_2 or at depth in its absence.

Table 9.

Integrated Activities Released (AR) and Integrated Release Rates (RR) of Co-60 and Ni-63 for various vertical sections of Core #2.

Depth (cm N)	Co-60 AR(nCi) ± 1 S	Co-60 RR(nCI/CM^2/yr) ± 1 S	Ni-63 AR(nCi) ± 1 S	Ni-63 RR(nCI/CM^2/yr) ± 1 S
2-4	0.0212 0.0014	0.0050 0.0003	0.0423 0.0257	0.0101 0.0061
6-7.5	0.0617 0.0023	0.0147 0.0005	0.1090 0.0243	0.0260 0.0058
12-14	0.9158 0.0050	0.2182 0.0012	0.4455 0.0189	0.1062 0.0045
22-24	0.0797 0.0023	0.0190 0.0005	0.0779 0.0230	0.0186 0.0055
38-40	0.0234 0.0014	0.0056 0.0003	N.D.	0.0000 0.0000

Core #4, Inconel-600: Table 10

Release rates of Co-60 from this Inconel-600 core are maximum at the uppermost sections (0.1 nCi/cm^2/yr at 6-8 cm) and fall off steadily with depth. There is a secondary maximum at 16.5-18.5 cm of 0.08 nCi/cm^2/yr. The Co-60 release rate values are smaller for Core #4 than its Inconel-600 predecessor, Core #5, with maximum values of 1.4 nCi/cm^2/yr at 14-16 cm. We are, perhaps, seeing a slowing down of the release rate with time as the metal surface corrodes. As with Core #2, the correlation of release rate with redox environment is not clear. It does seem evident, however, that release is accentuated above 20 cm depth.

The Ni-63 data from Core #4 compares well with the Co-60 data in that the same surface maximum (2.2 nCi/cm^2/yr) and secondary subsurface maximum (0.07 nCi/cm^2/yr) at 25.5-27.5 cm are observed. As with the cobalt data, these maxima are reduced from those measured after one year's deployment (13 nCi/cm^2/yr at 6-8 cm; ~3 nCi/cm^2/yr at 2-4 cm and 14-16 cm). Again, a possibility of diminishing release rate with time exists.

Table 10.

Integrated Activities Released (AR) and Integrated Release Rates (RR) of Co-60 and Ni-63 for various vertical sections of Core #4.

Depth (cm)	Co-60 AR(nCi) ± 1 S	Co-60 RR(nCI/CM^2/yr) ± 1 S	Ni-63 AR(nCi) ± 1 S	Ni-63 RR(nCI/CM^2/yr) ± 1 S
6-8 N	0.4207 0.0023	0.1003 0.0005	9.0865 0.0653	2.1653 0.0156
8-10 N	0.1477 0.0018	0.0352 0.0004	1.5923 0.0171	0.3795 0.0041
10-12 E	0.1829 0.0018	0.0436 0.0004	0.2401 0.0221	0.0572 0.0053
16.5-18.5 E	0.3685 0.0113	0.0878 0.0027	0.1973 0.0477	0.0470 0.0114
25.5-27.5 E	0.1495 0.0072	0.0356 0.0017	0.3063 0.0477	0.0730 0.0114
27.5-29.5 E	0.0851 0.0018	0.0203 0.0004	0.1725 0.0203	0.0411 0.0048
41-43.5 E	0.0581 0.0059	0.0138 0.0014	0.0477 0.0599	0.0114 0.0143

Core #6, Inconel-600: Table 11

Core #6 was recovered without its probe and extruded in 5 to 6 cm x 5 cm radius sections. The equations for calculating the AR and RR values are slightly different in that the activity need not be summed over many 2 mm thick shells as the previous cores were. The equations are:

$$AR = (A * D * B * V)/(F)$$

where:

AR = Activity released (nCi)

A = Activity measured in sediment aliquot (dpm/g wet wt)

D = Decay factor correcting from count date to deployment date

B = Sediment bulk density (g/cm^3 wet sediment)

V = Volume of 5 cm thick section

F = Conversion factor from dpm to nCi (1 nCi = 2.2×10^{-3} dpm)

and

$$RR = AR/(SA * T)$$

where:

RR = Release rate ($nCi/cm^2/yr$)

AR = Activity released (nCi)

SA = Total surface area of foil on probe (cm^2)

T = Elapsed time from deployment to extrusion (years)

AR and RR values for Ni-63 and Co-60 for 4 sections of Core #6 are shown in Table 11.

Table 11.

Integrated Activities Released (AR) and Integrated Release Rates (RR) of Co-60 and Ni-63 for various vertical sections of Core #6. (Values are means of several measurements ± 1 std. dev.)

Depth (cm)	Co-60		Ni-63	
	AR(nCi) ± 1 S	RR($nCI/CM^2/yr$) ± 1 S	AR(nCi) ± 1 S	RR($nCI/CM^2/yr$) ± 1 S
0-5	40 12	9.5 2.9	660 170	160 40
5-10	6.4 0.7	1.5 0.2	36 25	8.6 5.4
10-16	10 0.9	2.4 0.2	9.8 5.8	2.2 1.3
16-21	1.3 0.1	0.53 0.02	3.3 2.1	0.78 0.5

Core #6 provides an interesting comparison with Core #4 and Core #5 (1983 recovery). Release rates for both Co-60 and Ni-63 are extremely high in comparison to all other cores. Co-60 has a maximum of 9.5 $nCi/cm^2/yr$ in the 0-5 cm section and a secondary max at 10-16 cm of 2.4 $nCi/cm^2/yr$. These are about 30 to 100 times the maxima for Core #4. The relative difference is similar for Ni-63 (0-5 cm max = 160 $nCi/cm^2/yr$), but there is no secondary maximum. The release rate declines steadily with depth.

Despite the large error limits for the Core #6 data, it is still clear that bulk extrusion of a core captures more of the activity released from the foils than the syringe subsampling. Comparing the activities of the syringe subsamples closest to the foils (0.2 mm) from different syringes taken at the same depth one can observe as much as a factor of 20 variation in activity (see for example sections 6-8 E and 6-8 N of Core #4; Table 6). Not surprisingly, the bulk extrusion method provides samples that are far better averaged with respect to the inhomogeneity than is indicated by the replicate close in samples. This approach is preferred for estimates of integrated releases and rates. It cannot be used to determine migration rates, however.

The difference between the two approaches to sampling (bulk vs. syringe) is much greater in the upper 10 cm (Ni) to 15 cm (Co) (Figure 4). This is not easily explained except as heterogeneity in the distribution of this nuclide. It cannot arise from differences in the integration volumes, since the concentrations in the bulk samples are higher than the median values for the syringes. While the data are not ideal for comparison, there is no doubt as to the validity of the observed differences; the bulk activities in the 0-5 cm bulk sample are over an order of magnitude greater than the median values found in samples collected within 1 cm of the probes. This can only be explained as resulting from heterogeneity. In the 5-10 cm depth interval, geometric con-

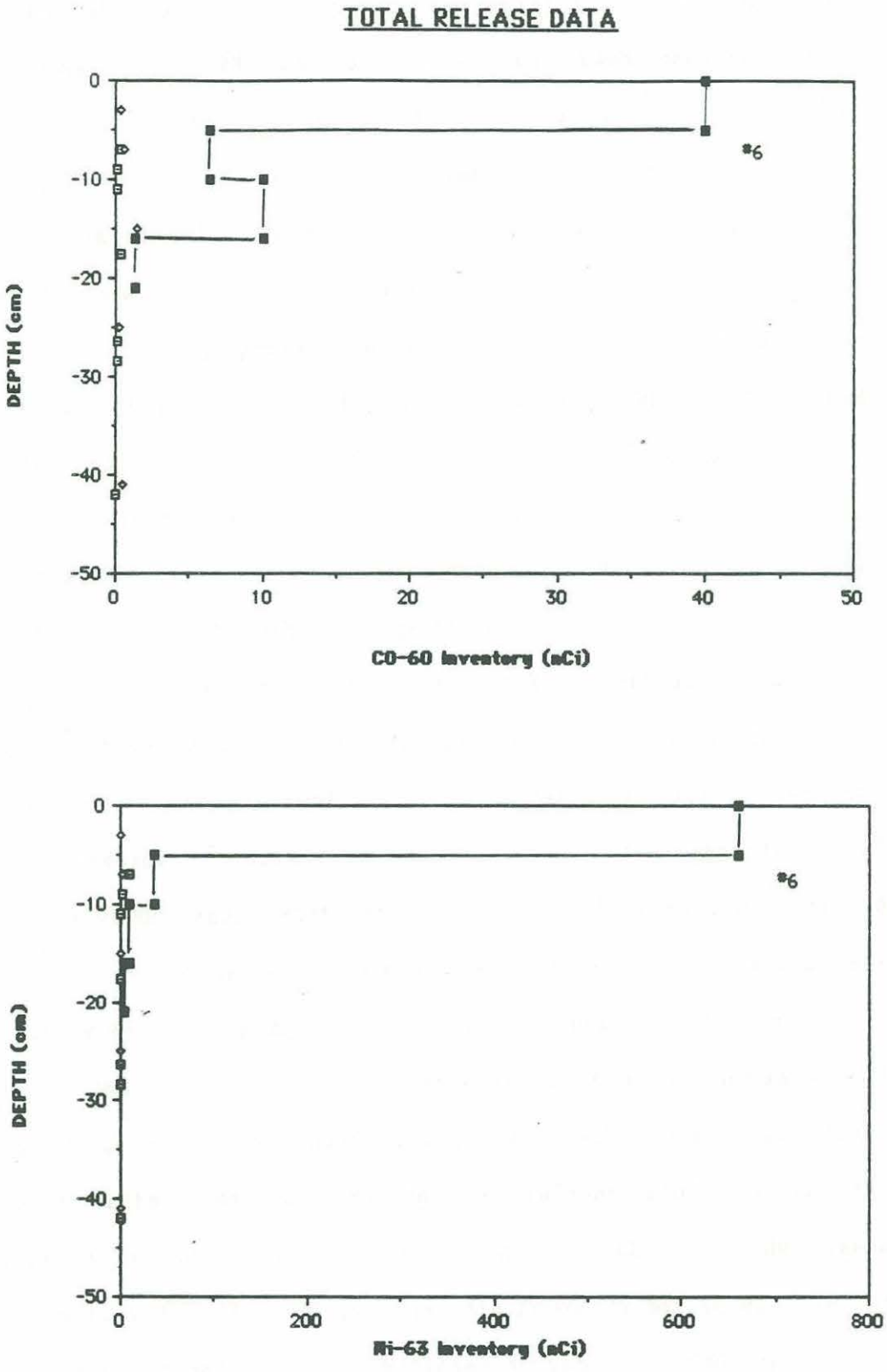

Figure 4. Inventories of Co-60 and Ni-63 plotted as a function of depth below the sediment-water interface. Shown for comparison are the data for the syringe sampled Inconel-600 cores (#4 and #5).

siderations can play a more important, but not exclusive, role in explaining the differing results. The syringe analyses themselves document the existence of marked heterogeneity on a mm scale, as well. For example, again the two sample sets analyzed from the 6-8 cm interval of core 4 differ over several sample intervals by as much as a factor of ~20 (cf. Table 6).

4. Redox Influences on Releases:

We believe the distributions observed in the bulk samples (Core #6) represent the most valid characterization of the release of Co-60 and Ni-63. This view is based on the observed variations in the syringe samples and the obviously better averaging achieved in the bulk sampling. This leads us to conclude that releases in the upper sediments are much greater than at depth. The resolution of the 5 cm samples is poor, but unambiguously supports the conclusion that it is in the O_2 environment that strongly enhanced release rates occur. Unfortunately, this is documented only for the Inconel-600 material; we lack the bulk sampling data to ascertain if the case is similar for the SS-347.

There are some second order patterns in the depth distributions of Ni and, especially, Co as determined from the syringe samples. We believed that these are real features, indicative of sediment processes, by virtue of their consistent occurrence. Four of the five cores sampled with syringes exhibit inventory maxima in the 10-20 cm depth interval (Figure 5). The bulk sampling also defines a maximum in the 10-15 interval for Co, but the 5 cm sample interval prevents resolution of the depth of occurrence. As in the shallowest samples, the inventory defined by the bulk sample is much larger. Only the core 3 syringe samples fail to define this feature with maximum inventories in the core occurring somewhat shallower. The enhanced releases of Co-60 implied

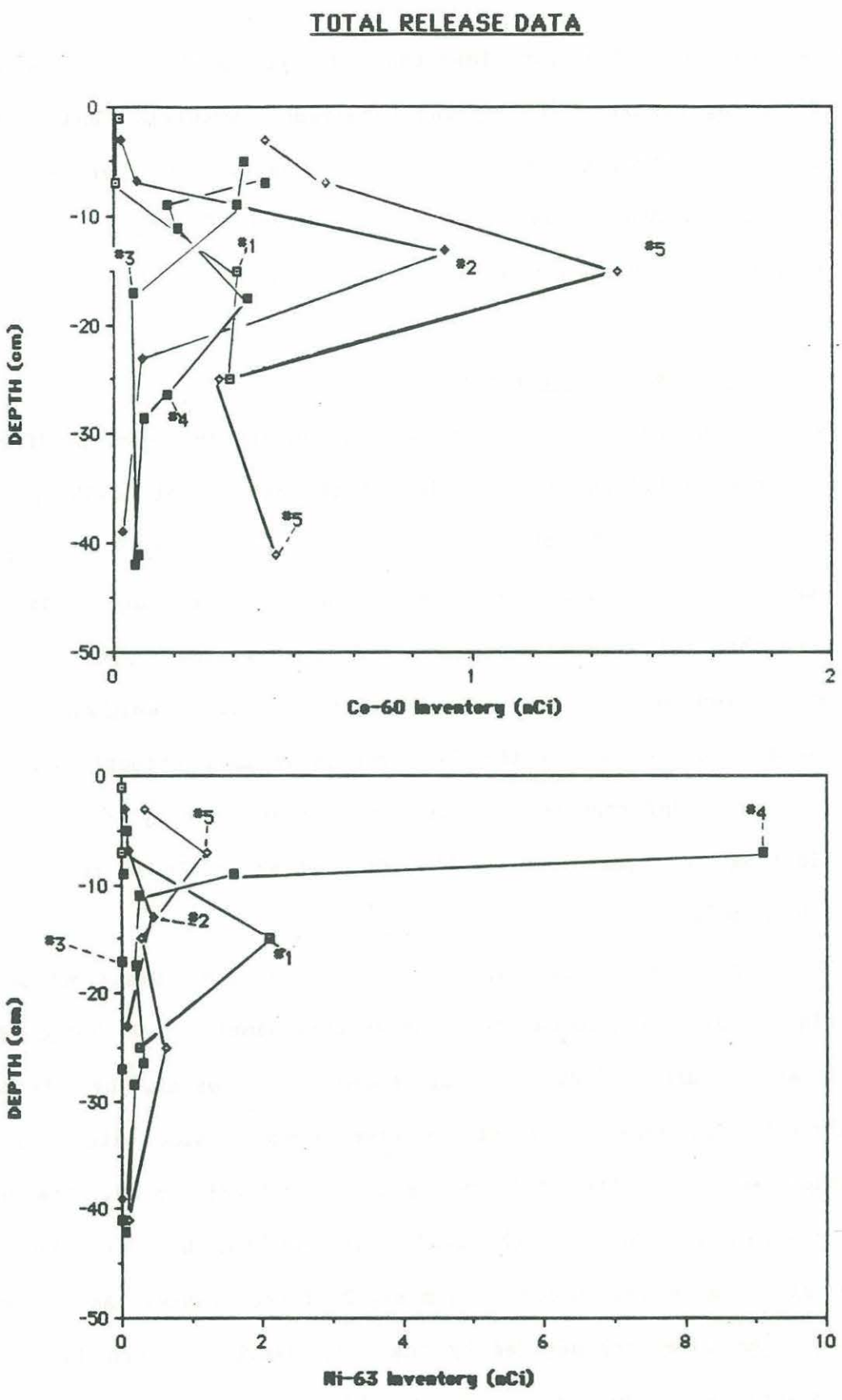

Figure 5. Inventories of Co-60 and Ni-63 for all syringe sampled cores plotted as a function of depth below the sediment-water interface. For reference, #4 and #5 are Inconel-600 foils; #1, #2, and #3 are SS-347 foils.

by the inventories in the 10-20 cm depth interval are mostly closely associated with the exhaustion of NO_3 through denitrification and the onset of MnO_2 reduction to Mn^{2+}. All of the cores have minimum, or near minimum, Co-60 inventories at depths of the order of 40 cm. Ni-63, however, does not exhibit a pattern consistent with Co-60. Maximum inventories of Ni-63 for the two Inconel cores are substantially shallower (6-9 cm) while inventories are fairly low in the 10-20 cm interval. Of the three SS-347 cores analyzed, only one (#1) exhibits a fairly strong maximum. For #2 and #3, it is either weak or absent.

In summary, the maxima at depth are very definitely secondary features when compared to the strongly enhanced near-surface release documented in the core 6 data. In the case of the Co-60 maximum at depth, we believe it to be real. The data are much more ambigious in the case of Ni-63. As regards the character of release rate with time, we do not believe that there is sufficient data to reach a sound conclusion. Without a comparison based on bulk samples, any conclusion would be questionable.

5. Migration Rates:

In extracting information on the rates of migration of Co and Ni within the sediment, it is necessary to use only the data from the syringe samples. Both of these isotopes are subject to extensive sorption on sediment surfaces and hence migrate through pore solutions at very slow rates. As a result, distributions are confined to short distances from the source where physical mixing processes, such as those at the sediment-water interface, are absent. It is also necessary to apply a model to the observed distributions in order to interpret the data as migration rates. Deriving diffusion coefficients from the data available requires, above all, assuming a functionality for

release rates. In modelling distributions we have assumed a constant rate of release. As discussed previously[1], the uncertainties in such an assumption make the values obtained order of magnitude estimates only. This situation remains the same for the values reported here. Further, these uncertainties preclude the development of a geometrically rigorous model and we have treated the distributions as two-dimensional. With these caveates in mind we have described the migration process with the equation:

$$C/C_o = \sqrt{\pi}\ \text{ierfc}[r/2\sqrt{Dt}].$$

Use of the data to define migration rates in terms of diffusion coefficients requires a fairly extensive data set and a core that does not appear subject to physical disturbance during coring and recovery. For this reason we focused our attention on Core #4. When the data are represented as r/2 Dt (derived from C/C_o and error function tables) vs. r, the data in the upper sediments are quite scattered, especially for Ni. The values, while poorly constrained, are consistent with diffusion coefficients of the order $1x10^{-10}$ cm^2/sec (cf. Figure 6). In deeper sediments (~15 cm), Co appears to fit the model reasonably well. The 25.5 and 41 cm sections define a linear trend consistent with D = $\sim 2x10^{-9}$ cm^2/sec, while the 16.5 cm data yield a somewhat higher value of $\sim 8x10^{-9}$ cm^2/sec. Ni is poorly constrained, but all the deeper sections are consistent with the range $1\text{-}3x10^{-9}$ cm^2/sec. Given the uncertainties in the applicability of the model, we believe that the results conservatively put the diffusion coefficient of both Ni and Co at about $1\text{-}5x10^{-9}$ cm^2/sec in the deeper sections. The higher values found at depth correspond to the zone of MnO_2 reduction. It is quite possible that the enhanced mobility of the released Co and Ni is the result of reduction of oxide surfaces in the sediment below the depth where NO_3 is completely

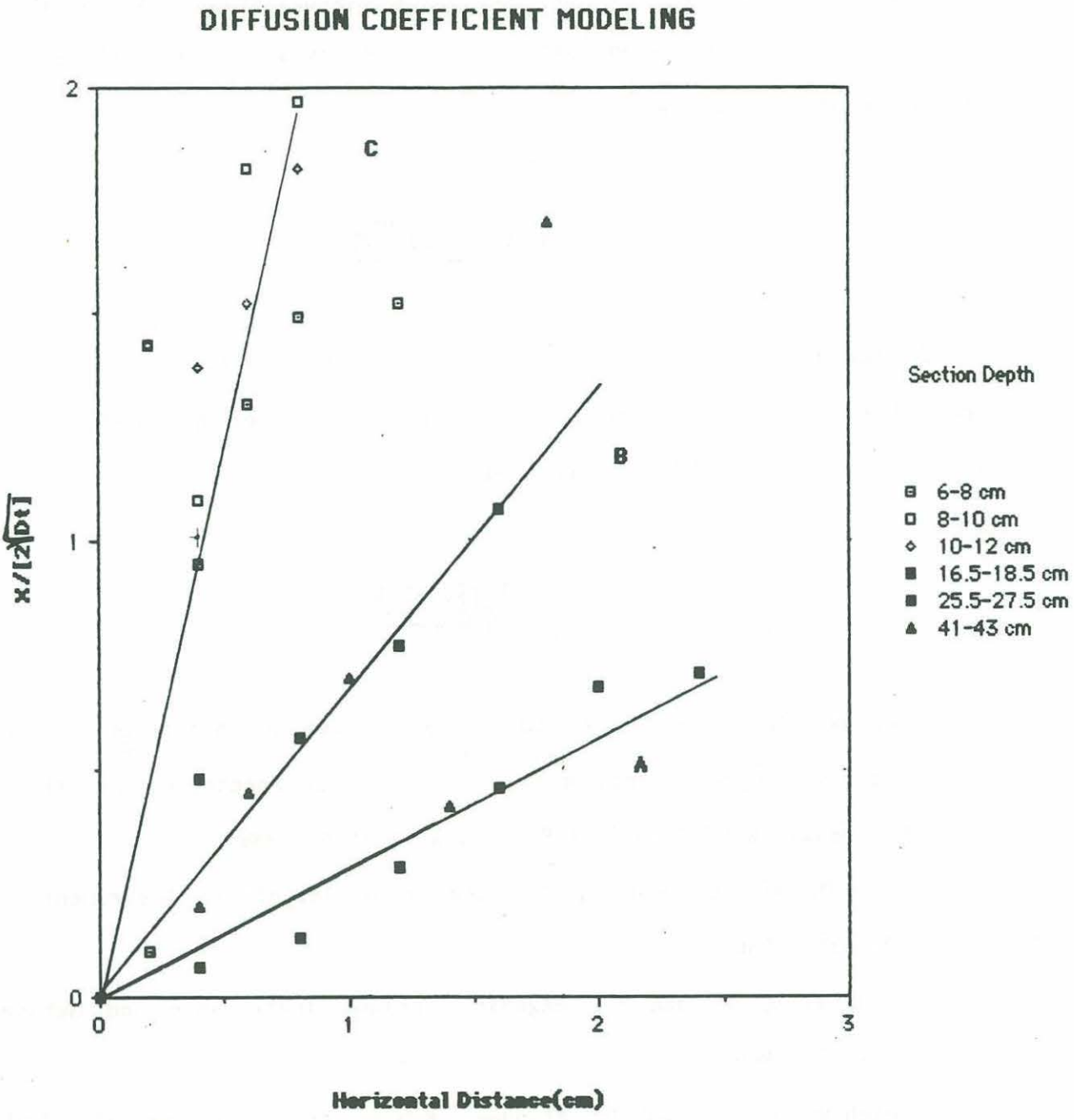

Figure 6. Parameterization of the activity vs. horizontal distance from the probe appropriate to the diffusion model used to obtain estimates of diffusion coefficients. The solid lines on the graph are representations of expected relationships for three different diffusion coefficients: A = 8.6×10^{-9} cm^2/sec; B = 1.6×10^{-9} cm^2/sec; C = 1.4×10^{-10} cm^2/sec.

consumed. Thus, despite the evidence of lower release rates under the reducing conditions at these depths (cf. preceding discussion), there is evidence of enhanced mobility consistent with expected changes in the surface properties of the sediment particles.

ACKNOWLEDGEMENTS

We would like to thank Hugh Livingston and the members of his research group for the use of their low level beta counting equipment, and Charlie Olson for the design of the windowless Ni-63 counter.

REFERENCES

(1) Sayles, F. L. and L. A. Ball, The Release and Migration of Activation Products from Corrosion-Resistant Metal Specimens in the Marine Sediments, WHOI Technical Report, WHOI-86-6, 1986.

(2) Lal, D. and D. Schink, The Review of Scientific Instruments, 31(4), 395-398, 1960.

(3) Noshkin, V. E. and E. DeAgazio, Nuclear Instruments and Methods, 39, 265-270, 1966.

(4) Volchok, H. L. and G. Planque, E.M.L. Procedures Manual, D-08-01 to D-08-07, 1982.

(5) Wilkinson, D. H., Ionization Chambers and Counters, Cambridge University Press, 1950.

APPENDIX

ENGINEERING DRAWINGS FOR THE WINDOWLESS Ni-63 G-M COUNTER

1 REQ

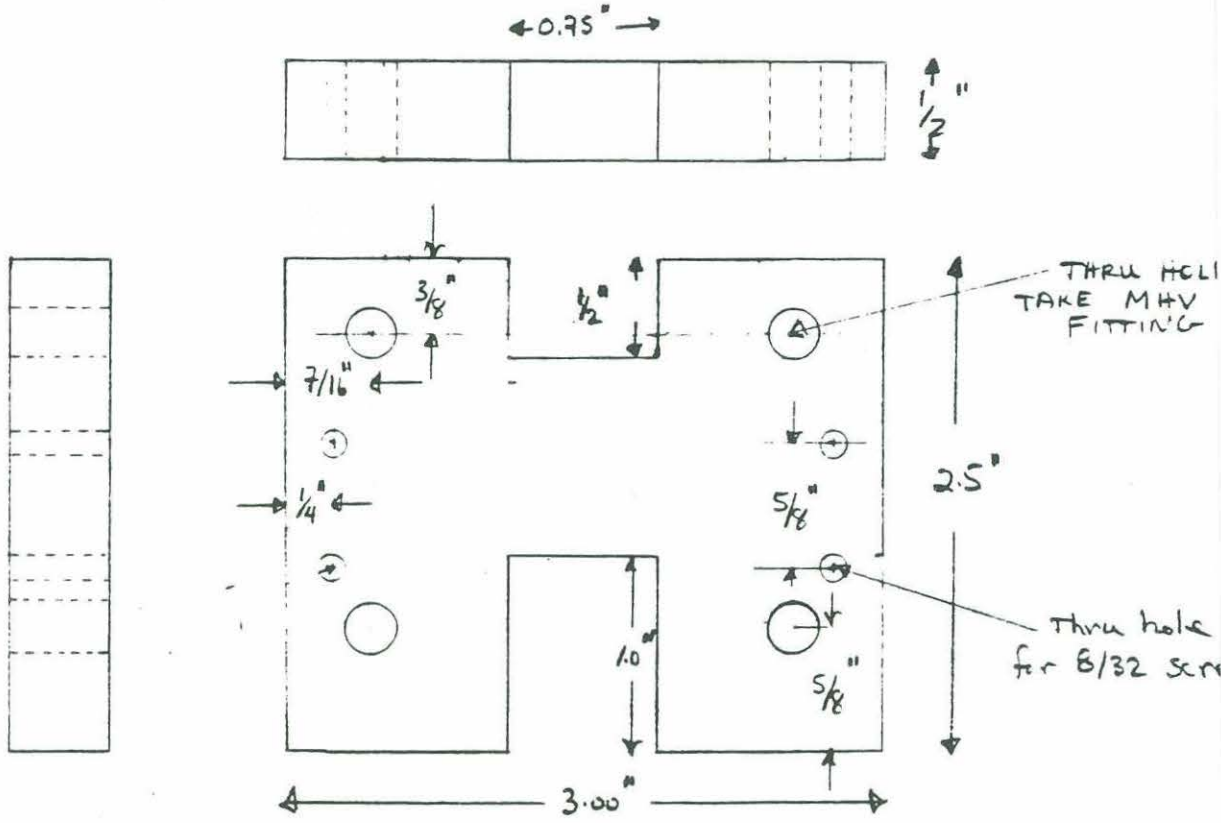

MAT: LUCITE

WOODS HOLE OCEANOGRAPHIC INSTITUTION WOODS HOLE, MASS. 02543	TITLE END PLATE
PROJ. _____ BY C OLSON	
SHEET _____ OF _____ DATE _____	

SP 11208A

2 REQ

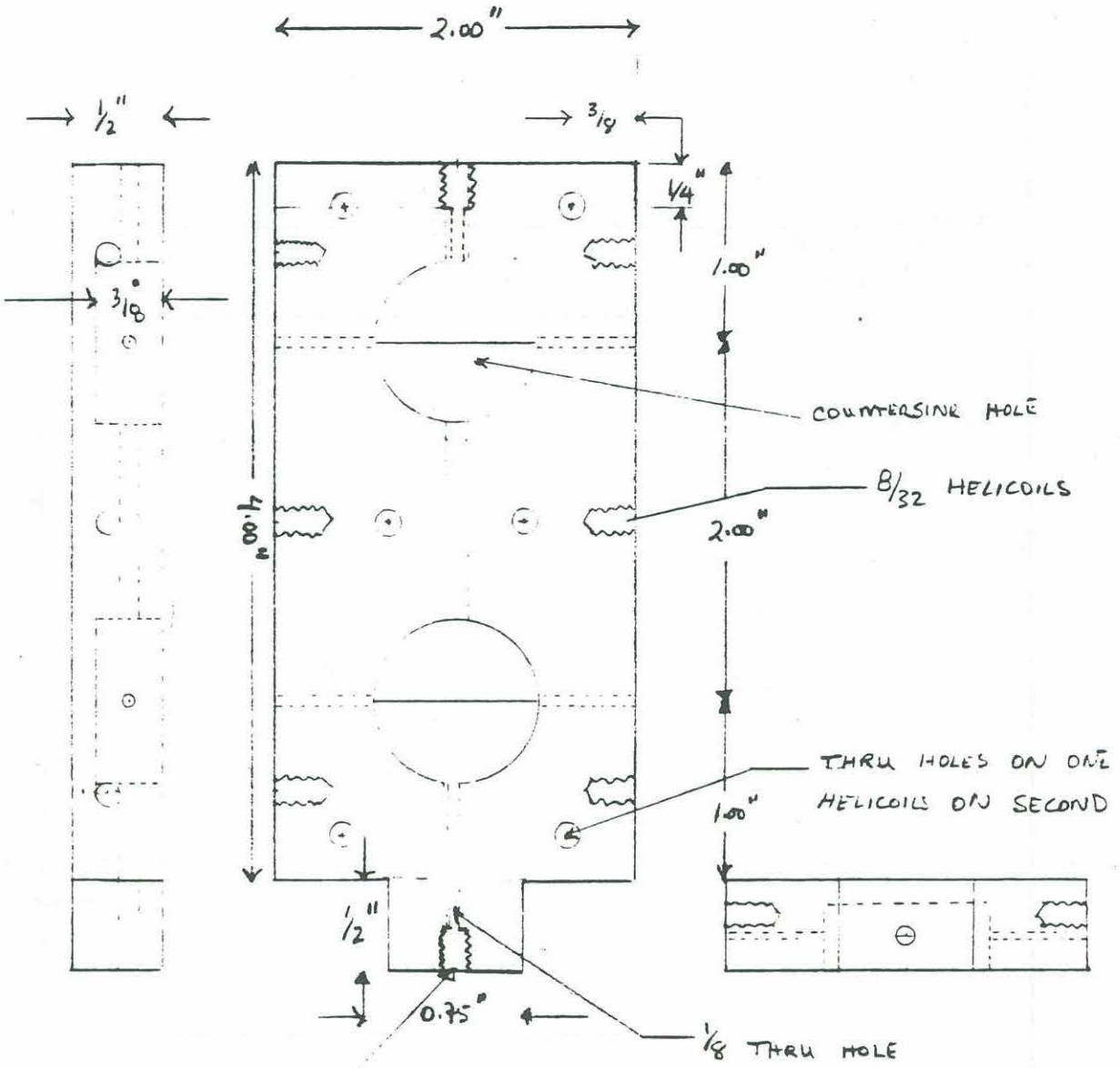

MAT LUCITE

WOODS HOLE OCEANOGRAPHIC INSTITUTION WOODS HOLE, MASS. 02543 PROJ. _____ BY C OLSON SHEET _____ OF _____ DATE _____	TITLE ANODE PLATE

SP 11206

2 REQ

HELICOILS FOR TAPPED PLATE

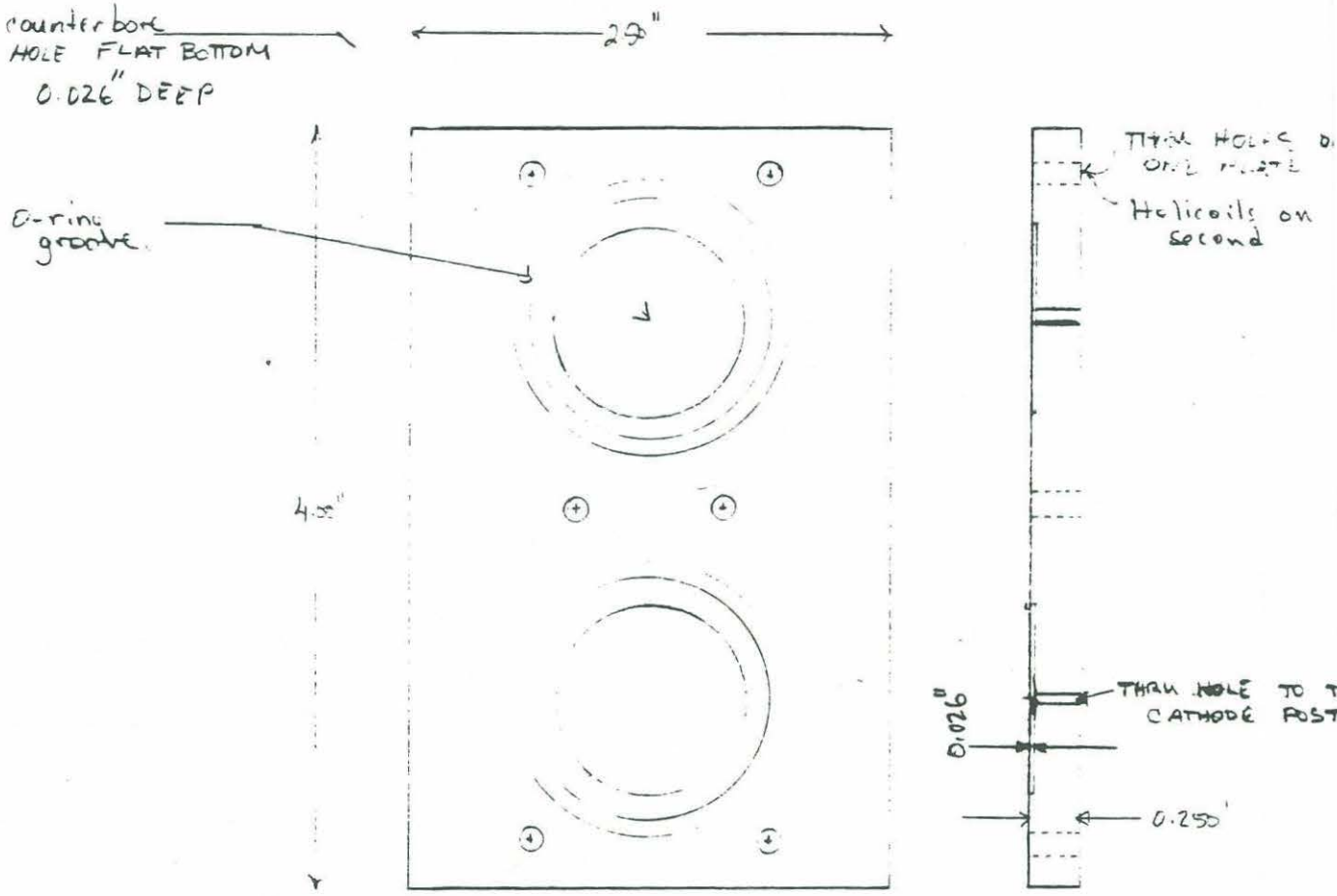

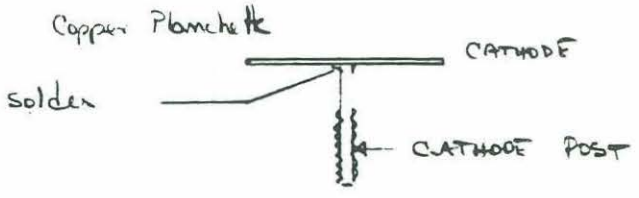

MAT. Lucite

WOODS HOLE OCEANOGRAPHIC INSTITUTION WOODS HOLE, MASS. 02543	TITLE CATHODE PLATE
PROJ. _____ BY C OLSON	
SHEET _____ OF _____ DATE _____	

SP 11208A

2 REQ

MIRROR IMAGES

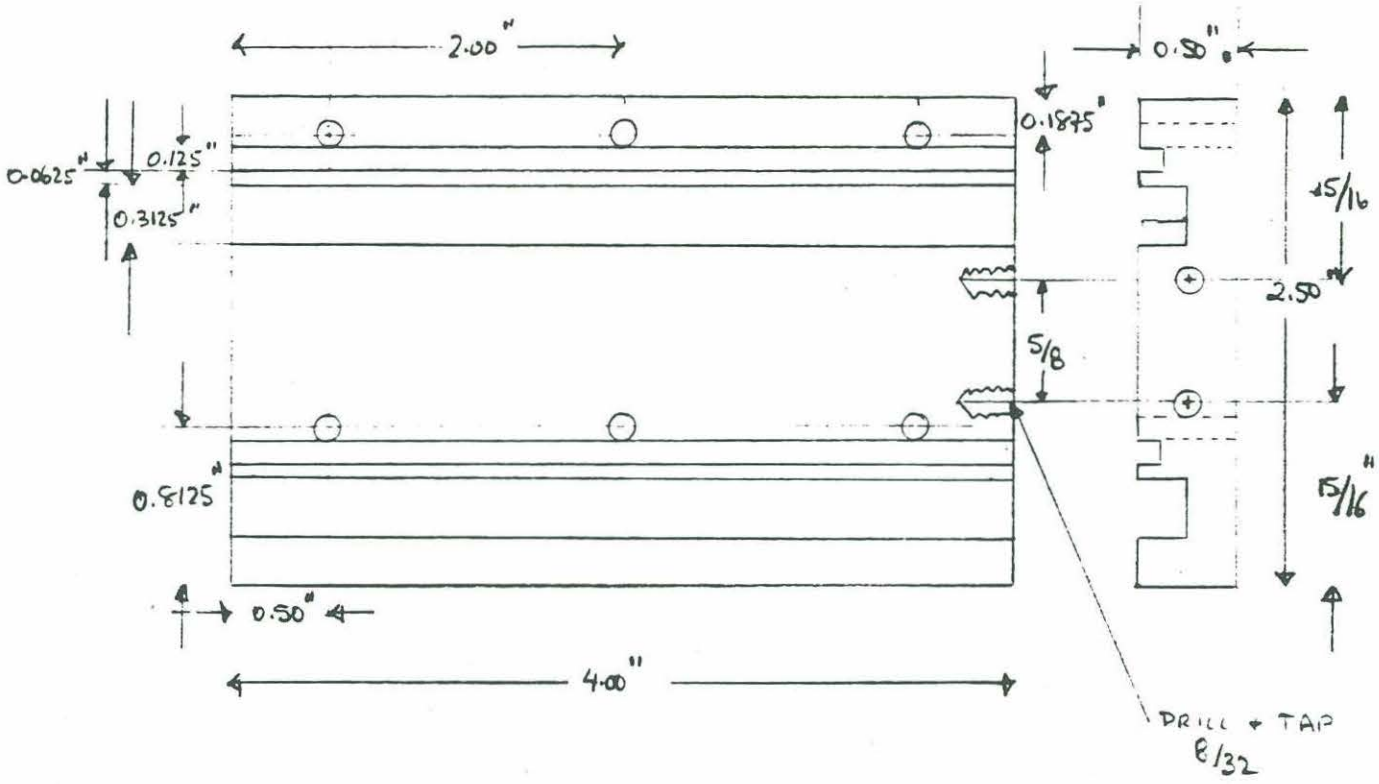

MAT: LUCITE

WOODS HOLE OCEANOGRAPHIC INSTITUTION WOODS HOLE, MASS. 02543 PROJ. _____ BY C OLSON SHEET _____ OF _____ DATE _____	TITLE SIDE PLATE

SP 1120BA

DOCUMENT LIBRARY

August 9, 1988

Distribution List for Technical Report Exchange

Attn: Stella Sanchez-Wade
Documents Section
Scripps Institution of Oceanography
Library, Mail Code C-075C
La Jolla, CA 92093

Hancock Library of Biology &
Oceanography
Alan Hancock Laboratory
University of Southern California
University Park
Los Angeles, CA 90089-0371

Gifts & Exchanges
Library
Bedford Institute of Oceanography
P.O. Box 1006
Dartmouth, NS, B2Y 4A2, CANADA

Office of the International
Ice Patrol
c/o Coast Guard R & D Center
Avery Point
Groton, CT 06340

Library
Physical Oceanographic Laboratory
Nova University
8000 N. Ocean Drive
Dania, FL 33304

NOAA/EDIS Miami Library Center
4301 Rickenbacker Causeway
Miami, FL 33149

Library
Skidaway Institute of Oceanography
P.O. Box 13687
Savannah, GA 31416

Institute of Geophysics
University of Hawaii
Library Room 252
2525 Correa Road
Honolulu, HI 96822

Library
Chesapeake Bay Institute
4800 Atwell Road
Shady Side, MD 20876

MIT Libraries
Serial Journal Room 14E-210
Cambridge, MA 02139

Director, Ralph M. Parsons Laboratory
Room 48-311
MIT
Cambridge, MA 02139

Marine Resources Information Center
Building E38-320
MIT
Cambridge, MA 02139

Library
Lamont-Doherty Geological
Observatory
Colombia University
Palisades, NY 10964

Library
Serials Department
Oregon State University
Corvallis, OR 97331

Pell Marine Science Library
University of Rhode Island
Narragansett Bay Campus
Narragansett, RI 02882

Working Collection
Texas A&M University
Dept. of Oceanography
College Station, TX 77843

Library
Virginia Institute of Marine Science
Gloucester Point, VA 23062

Fisheries-Oceanography Library
151 Oceanography Teaching Bldg.
University of Washington
Seattle, WA 98195

Library
R.S.M.A.S.
University of Miami
4600 Rickenbacker Causeway
Miami, FL 33149

Maury Oceanographic Library
Naval Oceanographic Office
Bay St. Louis
NSTL, MS 39522-5001

Marine Sciences Collection
Mayaguez Campus Library
University of Puerto Rico
Mayagues, Puerto Rico 00708

50272-101

REPORT DOCUMENTATION PAGE	1. REPORT NO. WHOI-88-31	2.	3. Recipient's Accession No.

4. Title and Subtitle

The Release and Migration of Activation Products from Corrosion-Resistant Metal Specimens in Marine Sediments

5. Report Date August 1988

6.

7. Author(s)

L.A. Ball and F.L. Sayles

8. Performing Organization Rept. No. WHOI-88-31

9. Performing Organization Name and Address

The Woods Hole Oceanographic Institution
Woods Hole, Massachusetts 02543

10. Project/Task/Work Unit No.

11. Contract(C) or Grant(G) No.

(C)

(G)

12. Sponsoring Organization Name and Address

13. Type of Report & Period Covered Technical Report

14.

15. Supplementary Notes

This report should be cited as: Woods Hole Oceanog. Inst. Tech. Rept., WHOI-88-31.

16. Abstract (Limit: 200 words)

This experiment was designed to measure the release and migration of the neutron-activated radionuclides, Ni-63, Co-60, and Fe-55, from two types of corrosion-resistant alloys, Incone1-600 and SS-347 into marine sediments. A previous report[1] described the experimental design in detail. To briefly summarize, on 11 August 1982 we deployed six 50 cm long probes at Deep Ocean Site 2 (DOS-2). Each probe held 5 metal specimens such that each specimen would be exposed to sediment at depths of approximately 3, 7, 15, 25, and 40 cm. Three probes held Incone1-600 specimens and three held SS-347. On July 17, 1983, we recovered one probe of each type of metal (probes #3 and #5). The extrusion and subsectioning procedure as well as the analytical methods and results from these cores were described in detail in the previous report. The integrated release rates for the three nuclides fell between 0.02-13 nCi/cm^2/yr for Incone1-600 and 0.007 to 0.36 nCi/cm2/yr for SS-347. Estimated diffusion coefficients were between 10^{-8} and 10^{-9} cm^2/sec for the three nuclides. We noted difficulty in detecting Fe-55 in general due to its short half life and consequently low specific activity. Measurement of Ni-63 in the core containing SS-347 foils was also difficult due to the low nickel content of this alloy and the relatively high detection limit of the LSC method.

17. Document Analysis a. Descriptors

1. Marine sediments
2. corrosion-resistance
3. activation products

b. Identifiers/Open-Ended Terms

c. COSATI Field/Group

18. Availability Statement

Approved for publication; distribution unlimited.

19. Security Class (This Report) UNCLASSIFIED

20. Security Class (This Page)

21. No. of Pages 37

22. Price

(See ANSI-Z39.18) *See Instructions on Reverse*

OPTIONAL FORM 272 (4-77)
(Formerly NTIS-35)
Department of Commerce